PNNL-14838



2004 Initial Assessments for the T and TX-TY Tank Farms Field Investigation Report (FIR): Numerical Simulations

Z. F. Zhang V. L. Freedman S. R. Waichler

September 2004



Prepared for the U.S. Department of Energy under Contract DE-AC06-76RL01830

DISCLAIMER

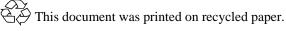
This report was prepared as an account of work sponsored by an agency of the United States Government. Neither the United States Government nor any agency thereof, nor Battelle Memorial Institute, nor any of their employees, makes **any warranty, express or implied, or assumes any legal liability or responsibility for the accuracy, completeness, or usefulness of any information, apparatus, product, or process disclosed, or represents that its use would not infringe privately owned rights. Reference herein to any specific commercial product, process, or service by trade name, trademark, manufacturer, or otherwise does not necessarily constitute or imply its endorsement, recommendation, or favoring by the United States Government or any agency thereof, or Battelle Memorial Institute. The views and opinions of authors expressed herein do not necessarily state or reflect those of the United States Government or any agency thereof.**

PACIFIC NORTHWEST NATIONAL LABORATORY operated by BATTELLE for the UNITED STATES DEPARTMENT OF ENERGY under Contract DE-ACO6-76RL01830

Printed in the United States of America

Available to DOE and DOE contractors from the Office of Scientific and Technical Information, P.O. Box 62, Oak Ridge, TN 37831-0062; ph: (865) 576-8401 fax: (865) 576-5728 email: reports@adonis.osti.gov

Available to the public from the National Technical Information Service, U.S. Department of Commerce, 5285 Port Royal Rd., Springfield, VA 22161 ph: (800) 553-6847 fax: (703) 605-6900 email: orders@ntis.fedworld.gov online ordering: http://www.ntis.gov/ordering.htm



PNNL-14838

2004 Initial Assessments for the T and TX-TY Tank Farms Field Investigation Report (FIR): Numerical Simulations

Z. F. Zhang V. L. Freedman S. R. Waichler

September 2004

Prepared for the U.S. Department of Energy under Contract DE-AC06-76RL01830

Pacific Northwest National Laboratory Richland, WA 99352

Summary

In support of CH2M HILL Hanford Group, Inc.'s (CHG) preparation of a Field Investigative Report (FIR) for the Hanford Site Single-Shell Tank Waste Management Area (WMA) T and TX-TY, a suite of numerical simulations of flow and solute transport was executed using the STOMP code to predict the performance of surface barriers for reducing long-term risks from potential groundwater contamination at the T and TX-TY WMA. The scope and parametric data for these simulations were defined by a modeling data package provided by CHG. This report documents the simulations involving 2-D cross sections through the T Tank Farm (T-106, T-105, and T-104) and the TX-TY Tank Farms (TX-105, TX-106, TX-107, and TX-108). Eight cases were carried out for the cross sections to simulate the effects of interim barrier, waterline leak, inventory distribution, and surface recharge on water flow and the transport of long-lived radionuclides (i.e., technecium-99 and uranium) and chemicals (i.e., nitrate and chromium). Fluid flow within the vadose zone is described by Richards' equation, whereas the contaminant transport is described by the conventional advective-dispersive transport equation with an equilibrium linear sorption coefficient (K_d) formulation.

For simulations with barriers, it was assumed that an interim barrier is in place by the year 2010. It was also assumed that, for all simulations, as part of tank farm closure, a closure barrier was in place by the year 2040. Placing a barrier is expected to significantly reduce infiltration of meteoric water and therefore arrival of contaminants at the water table. The modeling considers the estimated inventories of contaminants within the vadose zone and calculates the associated risk. It assumes that no tanks will leak in the future. Initial conditions for pressure head (and moisture) are established by allowing the vadose zone to equilibrate with an infiltration rate representative of natural infiltration for tank farm conditions. The data on infiltration rates with and without barriers are included in the discussion. Initial conditions for contaminant concentration are provided as part of inventory estimates for uranium, technetium-99, nitrate, and chromium. For moisture flow modeling, Neumann boundary conditions are prescribed at the surface with the flux equal to the recharge rate estimate. For transport modeling, a zero flux boundary is prescribed at the surface for uranium, technetium-99, nitrate, and chromium. The western and eastern boundaries are assigned no-flux boundaries for both flow and transport. The water table boundary is prescribed by water table elevations and the unconfined aquifer hydraulic gradient. No-flux boundaries are used for the lower boundary. Numerical results were obtained for compliance at the WMA boundary, 200 Areas boundary, exclusion boundary beyond the 200 Areas, and the Columbia River (DOE-RL 2000). Streamtube/analytical models were used to route computed contaminant concentrations at the water table to the downstream compliance points.

After the interim barrier was applied at 2010, saturation results indicate the soil desaturates gradually. The difference in saturation of the soil with and without the interim barrier was the largest at 2040, the time the closure barrier was applied. After this, the difference in saturation in the two cases became smaller with time. Generally, the solutes broke though faster if there was a waterline leak. A relatively small five-day leak (Case 4) had little effect on the peak concentration, while a large 20-yr leak (Case 3) increased the peak concentration significantly and reduced the solute travel in the vadose zone. The distribution of the inventory, either uniform or nonuniform, has little effect on peak arrival time; the peak concentrations of the conservative solutes varied by -6.9 to 0.2% for the T tank farm and by 11 to 49.4% for the TX tank farm. The reduction of the meteoric recharge before the barrier was applied led to less soil saturation, as expected, and thus longer solute travel time in the vadose zone and smaller peak

fenceline concentration. The effect on soil saturation lasted for about another 50 years after the barrier was applied at 2050. However, the reduced recharge rate affected the breakthough curve through the end of the simulation. The fenceline concentrations at the year 3000 were always higher for cases with reduced natural recharge than for those of the base case, which indicates that the fundamental impact of the reduced natural recharge is a smoothing of the breakthrough concentrations (lower peak concentration but higher tail concentration) at the compliance points.

Acronyms

ARH	Atlantic Richfield Hanford Comp
ASCII	American Standard Code for Information Interchange
bgs	below ground surface
BMI	Battelle Memorial Institute
BTCs	Break Through Curves
CA	Composite Analysis
CFEST	Coupled Fluid, Energy, and Solute Transport
CHG	CH2M HILL Hanford Group, Inc.
CR	Configuration report
DOE	U.S. Department of Energy
FIR	Field Investigation Report
GIS	Geographic Information System
IA	initial assessment
ICM	interim corrective measures
ILAW	Immobilized Low-Activity Waste
MDP	Modeling Data Package
NUREG	U.S. Nuclear Regulatory Commission regulation / Nuclear Regulatory Guide
ORP	Office of River Protection, U.S. Department of Energy
PNNL	Pacific Northwest National Laboratory
PNWD	Pacific Northwest Division
RCRA	Resource Conservation and Recovery Act
RPP	River Protection Project
SGM	Site-Wide Groundwater Model
SPLIB	A Library of Iterative Methods for Sparse Linear Systems
SST	Single-Shell Tank
STOMP	A flow simulator for Subsurface Transport Over Multiple Phases
TPA	The Tri-Party Agreement
WHC	Westinghouse Hanford Company
WMA	Waste Management Area

Table of Contents

Acronyms v 1.0 Introduction 1.1 2.0 Case Descriptions 2.1 3.0 Technical Approach 3.1 3.1 Overview 3.1 3.2 Modeling Data Package 3.2 3.2.1 Recharge Estimates 3.2
2.0 Case Descriptions 2.1 3.0 Technical Approach 3.1 3.1 Overview 3.1 3.2 Modeling Data Package 3.2
3.0 Technical Approach 3.1 3.1 Overview 3.1 3.2 Modeling Data Package 3.2
3.0 Technical Approach 3.1 3.1 Overview 3.1 3.2 Modeling Data Package 3.2
3.2 Modeling Data Package
3.2 Modeling Data Package
-
3.2.2 Vadose Zone Flow and Transport Properties
1.1.1 Stochastic Model for Macroscopic Anisotropy
3.2.3 Bulk Density and Retardation Coefficient
3.2.4 Diffusivity
3.2.5 Macrodispersivity
3.3 Input File Generation
3.3.1 Input File
3.3.2 Zonation File
3.3.3 Inventory File(s)
3.3.4 Two-Dimensional Cross-Section Concentrations
3.3.5 Inventory Scaling Factor
3.3.6 Fenceline Cumulative Mass Flux
3.3.7 Dimensional Scaling Factor and Fenceline Concentrations
3.4 Analytical Groundwater Transport Modeling
4.0 Simulation Results
4.1 Initial Conditions
4.2 Base Case (No-Action Alternative)
4.3 Barrier Alternative and No Waterline Leaks
4.4 Waterline Leak and No Interim Barrier
4.4.1 Case 3 No Barrier and Waterline Leak of 1 gpm for 20 yr
4.4.2 Case 4 No Barrier and 200,000 gal Waterline Leak
4.4.3 Effects of Waterline Leak
4.5 No Interim Barrier and Nonuniform Inventory Distribution
4.6 Base Case with Reduced Meteoric Recharge
4.6.1 Case 6, Base Case with 50 mm/yr Meteoric Recharge
4.6.2 Case 7 Base Case with 30 mm/yr Meteoric Recharge
4.6.3 Case 8, Base Case with 10 mm/yr Meteoric Recharge
4.6.4 Effects of Meteoric Recharge 4.25
4.7 Solute Mass Balance
5.0 Numerical Groundwater Transport Modeling Results
5.1 The Site-Wide Groundwater Model (SGM)
5.2 Flow and Transport Parameters for the SGM

5.3	Unit Source Analysis	5.6
5.4	Modeling Results	5.8
5.4	.1 Case 1: T Tank Farm	5.8
5.4	.2 Case 1: TX Tank Farm	5.12
6.0 Elec	ctronic Files	6.1
6.1	Source Coding	6.1
6.2	Geology and Initial Inventory	
6.3	Steady Flow Simulations	6.2
6.4	Coupled Vadose Zone and Unconfined Aquifer Modeling	6.2
6.5	Analytical Groundwater Transport Modeling	6.4
6.6	STOMP Execution and Post-Processing	6.5
7.0 Refe	erences	7.1

Figures

3.1	Rock/Soil Zonation for Cross Section Through T-104, T-105, and T-1063.7
3.2	Rock/Soil Zonation for Cross section Through TX-105, TX-106, TX-107, and TX-1083.7
3.3	Uniform and Nonuniform Distributions of Inventory
3.4	Converting a 3-D Volumetric Inventory to an Inventory of a 2-D Slice
3.5	Fenceline Aqueous Concentration Perpendicular to Flow Direction
3.6a	Comparison of BTCs of Tc-99 Simulated with 2- and 3-D
3.6b	Comparison of BTCs of U-238 with $K_{\rm d}{=}0.03$ mL/g Simulated with 2- and 3-D3.14
4.1	Aqueous-Phase Saturation at 20004.2
4.2	Aqueous-Phase Tc-99 Concentration at 2000 if Inventory Assigned as Uniform Distribution4.3
4.3	Aqueous-Phase U-238 Concentration at 2000 if Inventory Assigned as Uniform Distribution4.4
4.4	Aqueous-Phase NO ₃ Concentration at 2000 if Inventory Assigned as Uniform Distribution4.5
4.5	Aqueous-Phase Cr Concentration at 2000 if Inventory Assigned as Uniform Distribution4.6
4.6	Aqueous-Phase Tc-99 Concentration at 2000 if Inventory Assigned as Nonuniform Distribution.4.7
4.7	Aqueous-Phase U-238 Concentration at 2000 if Inventory Assigned as Nonuniform Distribution 4.8
4.8	Aqueous-Phase NO ₃ Concentration at 2000 if Inventory Assigned as Nonuniform Distribution4.9
4.9	Aqueous-Phase Cr Concentration at 2000 if Inventory Assigned as Nonuniform Distribution4.10
4.10	Aqueous-Phase Saturation at 2040 (100 mm/yr) for Cross Section T-104, -105, -1064.11
4.11	Aqueous-Phase Saturation at 2540 (0.1 mm/yr) for Cross Section T-104, -105, -1064.12
4.12	Aqueous-Phase Saturation at 3000 (3.5 mm/yr) for Cross Section T-104, -105, -1064.12
4.13	Effects of the Interim Cover on the Mean Saturation of the T Tank Farm4.15
4.14	Aqueous-Phase Saturation for Cross Section T-104, -105, -106 at the End of the
	Waterline Leak for Case 3
4.15	Variation of Water Flux at the Groundwater Table for Case 3 Due to the Pipeline Leak
4.16	Aqueous-Phase Saturation for Cross Section T-104, -105, -106 at the End of the
	Waterline Leak for Case 4
4.17	Effects of the Waterline Leaks on the Mean Saturation of T Tank Farm
4.18	Effects of Waterline Leaks on Tc-99 Concentration at the Fenceline of T Tank Farm4.20
4.19	Effects of Reduced Meteoric Recharge on the Mean Saturation of T Tank Farm4.25
4.20	Effect of Reduced Meteoric Recharge on Tc-99 Concentration at Fence Line of T Tank Farm4.25
5.1	Refined Composite Analysis Grid and 200 Areas
5.2	New Interpretation of the Basalt Outcrop Locations for Post-Hanford Flow Conditions
5.3	Map of SGM Hydrogeologic Units Containing Water Table in March 19995.4
5.4	Hydraulic Conductivity Distribution
5.5	Post-Hanford Operations, Steady-State Potentiometric Surface for SGM, and Streamtrace
5 (Along Peak Concentration Pathways
5.6	BTCs Simulated by CFEST Site-Wide Model for T-Farm Case 1

5.7	Composite SGM Results for Case 1 for the East Flow Path	.5.10
5.8	Composite SGM Results for Case 1 for the North Flow Path	.5.11
5.9	BTCs Simulated by CFEST Model for TX-Farm Case 1 for East and North Flow Paths	.5.13
5.10	Composite SGM Results for Case 1, TX Tank Farm, for East Flow Path	.5.14
5.11	Composite SGM Results for Case 1, TX Tank Farm, for the North Flow Path	.5.15

Tables

3.1	Time Estimates for Interim and Closure Barriers at the T and TX-TY Tank Farms and Corresponding Recharge Estimates
3.2	Composite van Genuchten-Mualem Parameters for Various Strata at the T and TX-TY Tank Farms
3.3	Macroscopic Anisotropy Parameters Based on the Polmann Equations for Strata at the T and TX-TY WMA
3.4	Effective Parameter Estimates for the Product of Bulk Density and Retardation Coefficient for U-238 at T and TX-TY WMA
3.5	Nonreactive Macrodispersivity Estimates for Strata at T and TX-TY WMA
3.6	The Inventory Scaling Factors
4.1	Total Inventory for Tc-99, U-238, NO ₃ , and Cr4.3
4.2	Mean Aqueous-Phase Saturation
4.3	Peak Concentrations and Arrival Times at the Fenceline for Case 14.14
4.4	Peak Concentrations and Arrival Times at the Fenceline for Case 24.15
4.5	Peak Concentrations and Arrival Times at the Fenceline for Case 34.17
4.6	Peak Concentrations and Arrival Times at the Fenceline for Case 44.19
4.7	Peak Concentrations and Arrival Times at the WMA Fenceline for Case 54.21
4.8	Peak Concentrations and Arrival Times at the WMA Fenceline for Case 64.22
4.9	Peak Concentrations and Arrival Times at the WMA Fenceline for Case 74.23
4.10	Peak Concentrations and Arrival Times at the WMA Fenceline for Case 84.24
4.11	Predicted Peak Tc-99 Flux, Arrival Time, and Cumulative Mass4.26
4.12	Predicted Peak U-238 Flux, Arrival Time, and Cumulative Mass4.27
4.13	Predicted Peak NO ₃ Flux, Arrival Time, and Cumulative Mass
4.14	Predicted Peak Cr Flux, Arrival Time, and Cumulative Mass
4.15	Predicted Peak Tc-99 Aqueous Concentrations and Arrival Time Summary4.29
4.16	Predicted Peak U-238 Aqueous Concentrations and Arrival Time Summary4.30
4.17	Predicted Peak NO ₃ Aqueous Concentrations and Arrival Time Summary4.31
4.18	Predicted Peak Cr Aqueous Concentrations and Arrival Time Summary4.32
4.19	STOMP Mass Balance Within the 2-D Slice for Tc-99
4.20	STOMP Mass Balance Within the 2-D Slice for U-238
4.21	STOMP Mass Balance Within the 2-D Slice for NO ₃
4.22	STOMP Mass Balance Within the 2-D Slice for Cr
5.1	Travel Distances, Times, and Average Velocities for Streamtube Model at T Farm5.7
5.2	Travel Distances, Times, and Average Velocities for Streamtube Model at TX Farm5.7
5.3	Peak Tc-99 Concentrations at the 200 West Eastern Boundary, Exclusion Boundary, and Columbia River for Case 1, T Tank Farm

5.4	Peak Tc-99 Concentrations at the 200 West Eastern Boundary, Exclusion Boundary,	
	and Columbia River for Case 1, TX Tank Farm	5.16
6.1	Source Code Directory	6.1
6.2	Steady Flow Initial Condition Files	6.2
6.3	Coupled Vadose Zone and Unconfined Aquifer Modeling Files	6.3
6.4	Analytical Groundwater Transport Modeling Files	6.4